Downloaded from UvA-DARE, the institutional repository of the University of Amsterdam (UvA)
http://hdl.handle.net/11245/2.30110

File ID	uvapub:30110
Filename	135712y.pdf
Version	unknown

SOURCE (OR PART OF THE FOLLOWING SOURCE):

Type	article
Title	Localized and delocalized plasmon excitations in single wall carbon nanotubes
Author(s)	T. Pichler, M. Knupfer, M.S. Golden, J. Fink, A. Rinzler, R.E. Smalley
Faculty	UvA: Universiteitsbibliotheek
Year	1998

FULL BIBLIOGRAPHIC DETAILS:
http://hdl.handle.net/11245/1.426322

Copyright

It is not permitted to download or to forward/distribute the text or part of it without the consent of the author(s) and/or copyright holder(s), other than for strictly personal, individual use, unless the work is under an open content licence (like Creative Commons).

UvA-DARE is a service provided by the library of the University of Amsterdam (http://dare.uva.nl)
(pagedate: 2014-11-27)

Localized and Delocalized Electronic States in Single-Wall Carbon Nanotubes

T. Pichler, M. Knupfer, M. S. Golden, and J. Fink
Institut für Festkörper- und Werkstofforschung Dresden, Postfach 270016, D-01171 Dresden, Germany

A. Rinzler and R. E. Smalley
Center for Nanoscale Science and Technology, Rice Quantum Institute, Departments of Chemistry and Physics, Ms-100, Rice University, P.O. Box 1892, Houston, Texas 77251
(Received 18 December 1997)

We present momentum-dependent measurements of the density response function of bulk samples of purified single-wall nanotubes probed by electron energy loss spectroscopy. Carbon nanotubes support excitations between both delocalized and localized electronic states. The π plasmon exhibits a $\mathbf{q}$ dependence similar to that of the graphite plane, signaling the graphitelike nature of the nanotube electron system along the tube axis. In contrast, the interband excitations between the singularities in the nanotube electronic density of states observed at low energy have vanishingly small dispersion in $\mathbf{q}$, and can be used to show that our samples contain significant quantities of semiconducting and metallic single-wall nanotubes. [S0031-9007(98)06196-1]

PACS numbers: 71.20.Tx, 73.20.Mf, 78.20.Ci

Carbon nanotubes are a promising extension of the growing family of novel fullerene-based materials, and represent ideal building blocks for nanoengineering as a result of their special electronic [1,2] and mechanical [3] properties. Nanotubes can be envisaged as rolled-up graphene sheets which are capped with fullerenelike structures. Their electronic properties are predicted to vary depending upon the wrapping angle and diameter of the graphene sheet, thus giving either metallic or semiconducting behavior [4–6].

Single wall nanotubes (SWNTs) are the best system in which to investigate the intrinsic properties of this new material class. However, macroscopic nanotube samples generally contain a distribution of tubes with different diameters and chirality and thus present the experimentalist with an averaged picture of their properties. One approach which has been successfully used to overcome this problem is to study individual SWNTs. Consequently transport measurements [7] and scanning tunneling spectroscopic (STS) and topographic (STM) studies of *single* nanotubes [8] have done much in the recent months to advance our knowledge regarding the properties of SWNTs, for example, by experimentally verifying the remarkable relationship between nanotube geometry and their electronic properties [8]. In addition, spatially resolved electron energy-loss spectroscopy (EELS) has been performed on individual multiwall nanotubes (MWNT) [9–11] or on a single bundle of SWNTs [12].

Nevertheless, there is still a paucity of experimental information regarding the electronic properties of purified SWNTs, in particular, using methods which can be applied to macroscopic samples. Combined electron spin resonance, microwave, and dc resistivity measurements [13] have led to the conclusion that bulk SWNT material is metallic. Resonant Raman measurements have been interpreted in terms of the vibrational modes of nonchiral "armchair" SWNTs [14], which would appear to be in contrast to the results from scanning tunneling microscopy in which chiral as well as nonchiral (armchair and "zigzag") nanotubes were positively identified [8].

In this contribution we present high resolution momentum-dependent EELS of purified SWNTs, in which we show that they support two types of electronic excitations. The first group of excitations are nondispersive, whereby their energy position is characteristic of the separation of the van Hove singularities in the electronic density of states (DOS) of the different types of nanotubes. The second type of excitation shows considerable dispersion, which parallels that observed in the graphite plane, and is related to a collective excitation of the π-electron system polarized along the nanotube.

SWNTs were produced by a laser vaporization technique [15]. The material consists of up to 60% SWNTs with approximately 1.4 nm mean diameter and was purified as described in Ref. [16]. Freestanding films for EELS of thickness about 1000 Å were prepared on standard copper microscopy grids via vacuum filtration of a nanotube suspension in a 0.5% surfactant (Triton X100) solution in deionized water, with a SWNT concentration of $\sim$0.01 mg/ml. The surfactant was then rinsed off, and the grid was transferred into the spectrometer. EELS was carried out in a purpose-built high-resolution spectrometer [17] which combines both good energy *and* momentum resolution. For the data shown here, an energy and momentum resolution of 115 meV and 0.05 Å^{-1} was chosen. Unlike many electron spectroscopies, this method has the advantage of being volume sensitive. In addition, by setting the energy loss to zero, we are able to characterize the films using electron diffraction. A Bragg spectrum consistent with the triangular SWNT lattice as published in Ref. [15] was found.

 © 1998 The American Physical Society

In Fig. 1 we show the loss function $[\mathrm{Im}(-1/\epsilon(q,E))]$ for the purified SWNTs measured as a function of **q**, after the subtraction of the quasielastic line and the effects of multiple scattering. The inset shows the loss function for $q = 0.15$ Å^{-1} over a wide energy range, in which the π plasmon, which represents the collective excitation of the π-electron system, can be clearly seen at an energy of 5.2 eV, and the $\sigma + \pi$ plasmon (the collective excitation of all valence electrons) at 21.5 eV. These values for SWNTs are in agreement with the spatially resolved EELS data mentioned above [12] and confirm theoretical predictions that the π plasmon should occur in the energy range of 5–7 eV in the EELS of these materials [18–20]. Figure 1 shows that we are able to reliably measure the **q** dependence of excitations in SWNTs with energies as low as 0.5 eV, which will be shown in the following to be vital to the understanding of their dielectric response. We note that these data provide a wealth of information not accessible in spatially resolved EELS measurements, in which the study of momentum dependence is excluded and the broad quasielastic tail of the direct beam has only allowed the extraction of reliable information for energies above ~3 eV [9–12].

The loss function measured in an EELS experiment is a direct probe of the collective excitations of the system under consideration. Thus, by definition, all peaks in the measured loss function should be considered as plasmons. These peaks can, however, have different origins such as charge carrier plasmons and interband or intraband excitations. From the q dependence of the loss function, we can distinguish directly between features arising from localized or delocalized electronic states. Localized states give rise to a vanishingly small dispersion of peaks in the loss function as has been observed, for example, for the features related to the interband excitations and both the π and $\pi + \sigma$ plasmons of C_{60} [21]. On the other hand, excitations between delocalized states generally exhibit a band structure dependent dispersion relation. Bearing these points in mind, the identification of excitations between localized and delocalized states in SWNTs is straightforward. At low momentum transfer, features in the loss function are visible at about 0.85, 1.45, 2.0, 2.55, 3.7, 5.2, and 6.4 eV whose origin lies in the π electron system of the SWNTs [22]. However, two distinct behaviors of these features as a function of **q** are observed. The π plasmon disperses strongly from 5.2 eV at $q = 0.1$ Å^{-1} to 7.4 eV at $q = 0.6$ Å^{-1}, whereas all the other peaks have a vanishingly small dispersion.

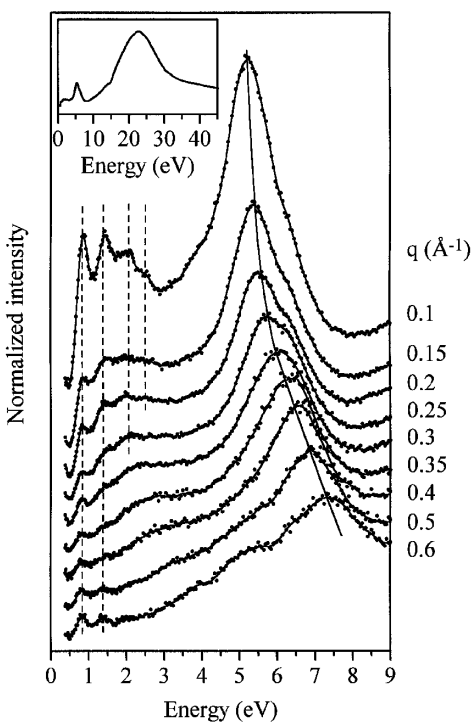

FIG. 1. The loss function of purified SWNTs from EELS in transmission for the different **q** values shown. The contributions from the elastic peak have been subtracted. The inset contains the loss function over an extended energy range for $q = 0.15$ Å^{-1}, showing the π plasmon and the $\pi + \sigma$ plasmon at around 5 and 22 eV, respectively.

The momentum dependence of the peaks in the loss function resulting from the four lowest-lying interband transitions of the SWNTs, as well as those of the π and $\pi + \sigma$ plasmons, is shown in Fig. 2. For comparison we also show the dispersion of the π and $\pi + \sigma$ plasmons of graphite with **q** parallel to the planes. In low-dimensional systems, the nature of the plasmon excitations depends on their polarization. This has been shown, for example, for oriented transpolyacetylene, whereby a dispersive plasmon is only visible in the one-dimensional direction [23].

Thus, in combination with the well-known one dimensionality of nanotubes, we arrive at the following picture: the nondispersive peaks in the loss function are due to excitations between localized states polarized *perpendicular* to the nanotube axis and thus resemble molecular interband transitions such as those of C_{60}. In contrast, the π plasmon (at 5.2 eV for low **q**) represents a plasma oscillation of delocalized states polarized *along* the nanotube axis. As can be seen from Fig. 2, the dispersion relations of both the π and the $\pi + \sigma$ plasmons in SWNTs and graphite are very similar, which confirms the graphitic nature of the axial electron system in carbon nanotubes.

By carrying out a Kramer-Kronig analysis (KKA) of the loss function we can derive the real (ϵ_1) and imaginary parts (ϵ_2) of the dielectric function. The results of such a KKA are depicted in the upper panels of Fig. 3 for C_{60}, SWNTs, and graphite (measured in the plane). In the lowest panel the corresponding real part of the optical conductivity is plotted, whereby $\sigma_r(E) = (E/\hbar)\epsilon_o\epsilon_2$ is a measure of the joint density of states. For the KKA of the SWNTs the loss function was normalized using an estimated $\epsilon_r(q,0)$ [24]—a procedure which has been used successfully in the past for graphite [25,26].

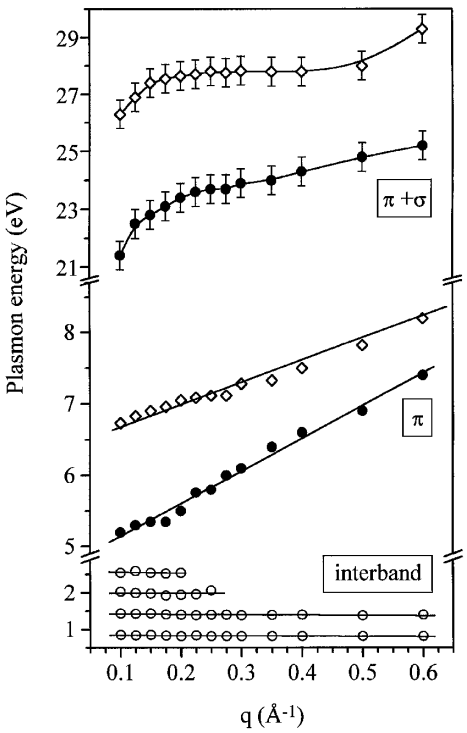

FIG. 2. The dispersion of the π, $\pi + \sigma$ plasmons (•), and of the features arising from interband transitions between localized states (∘) in purified SWNTs from EELS in transmission measurements. When invisible, the error bars are within the size of the symbols. For comparison the dispersion of the π and $\pi + \sigma$ plasmons in graphite for momentum transfer parallel to the planes is also shown as (◇).

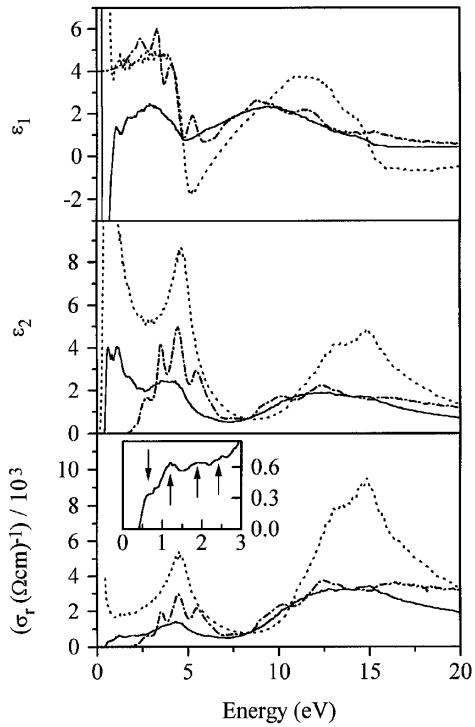

FIG. 3. The real and imaginary parts of the dielectric function (upper panels) and the real part of the optical conductivity (σ_r) at low momentum transfer: SWNTs (−) at $q = 0.1$ Å^{-1}, C_{60} (− · −) and graphite [polarized in plane (· · ·)] at $q = 0.15$ Å^{-1}, respectively. The inset shows σ_r for the four lowest-lying interband transitions of SWNTs in an expanded range.

In general, the optical conductivity of these sp^2 conjugated carbon systems shows peaks due to transitions between the (π/σ) and the $(\pi^\star/\sigma^\star)$ electronic states. In C_{60} these peaks are very pronounced which is consistent with the high symmetry of the molecule and the weak, van der Waals interactions in the solid state [27], making C_{60} a prototypical zero-dimensional solid. In graphite three broad features are observed at 4.5 ± 0.05, 13 ± 0.05, and 15 ± 0.05 eV. Their breadth is an expression of the bandlike nature of the electronic states in the graphite plane. For the SWNTs we also find three broad features at energies slightly lower than those in graphite—i.e., 4.3 ± 0.1, 11.7 ± 0.2, and 14.6 ± 0.1 eV. Importantly, the optical conductivity of the SWNTs also exhibits additional structures at low energy. This region is shown in detail in the inset of Fig. 3, where three pronounced interband transitions are seen at energies of 0.65 ± 0.05, 1.2 ± 0.1, and 1.8 ± 0.1 eV. Three further features, which are less pronounced, are located at 2.4 ± 0.2, 3.1 ± 0.2, and 6.2 ± 0.1 eV.

As the SWNT data in the lowest panel (and inset) of Fig. 3 represent joint densities of states, we can directly relate the energy position of the features with the energetic separation of the one-dimensional van Hove singularities in their electronic density of states. It is known from x-ray diffraction that these samples of SWNTs have a narrow diameter distribution around a mean value of 1.4 nm [15]. The fact that we observe well defined nondispersive features in the EELS data confirms a narrow diameter distribution, as otherwise the sheer number of energetically different interband transitions would wash out all fine structure in this energy range, both in the loss function or in the optical conductivity.

The feature at lowest energy (0.65 eV) is unambiguous—for the nanotube diameter range relevant here, only the gap transition in semiconducting nanotubes is predicted to lie at such low energies [4–6]. STS experiments on single nanotubes, which were characterized using STM, have recently confirmed these predictions [8]. The peak appearing in the optical conductivity at 1.8 eV, corresponds directly to the "gap" between the DOS singularities straddling E_F which have been observed experimentally in STS of metallic chiral and zigzag tubes [8]. Thus the feature at 1.8 eV in the optical conductivity clearly originates from metallic nanotubes. The origin of the feature at 1.2 eV is less clear-cut. This energy corresponds to the separation observed between the second pair of singularities in semiconducting, chiral nanotubes [8], but is also consistent with a predicted energetic separation of the first pair of singularities in metallic, armchair nanotubes [14]. For the features at higher energies, an

assignment based upon a discussion of particular nanotubes becomes less secure due to the large number of possible optically allowed transitions.

In summary, we have demonstrated that momentum-dependent high-resolution EELS in transmission measurements of SWNTs show that they represent a textbook example of a system supporting both excitations between localized and delocalized electronic states. Along the nanotube axis SWNTs support a π plasmon between delocalized states whose dispersion relation is very similar to that of the graphite plane, proving the graphitic nature of the electronic system in this direction. At low energies, nondispersive features are observed whose energy location in the real part of the optical conductivity is directly related to the energy separation of the DOS singularities in the nanotubes. Thus, assuming the matrix elements governing the EELS transitions for different nanotubes to be comparable, we prove the presence of a significant proportion of semiconducting nanotubes in these bulk samples in addition to the metallic nanotubes inferred from other measurements [14,15]. These data show that EELS in transmission offers a source of information regarding the character (semiconducting/metallic) of carbon nanotubes in *bulk, macroscopic* samples—which makes it an ideal complement to spatially resolved measurements of individual SWNTs. Moreover, the differences in **q** dependence of the features polarized along and perpendicular to the nanotube axis make momentum-dependent EELS an ideal probe of anisotropies in oriented bulk samples of SWNTs in the future.

T. P. thanks the European Union for funding under the "Training and Mobility of Researchers" program. The work at Rice was supported by the National Science Foundation (DMR9522251), the Advanced Technology Program of Texas (003604-047), and the Welch Foundation (C-0689).

[1] S. Saito, Science **278**, 77 (1997).
[2] L. Chico *et al.*, Phys. Rev. Lett. **76**, 971 (1996).
[3] E. W. Wong, P. E. Sheehan, and C. M. Lieber, Science **277**, 1971 (1997).
[4] J. W. Mintmire, B. I. Dunlop, and C. T. White, Phys. Rev. Lett. **68**, 631 (1992).
[5] N. Hamada, S. I. Sawada, and A. Oshiyama, Phys. Rev. Lett. **68**, 1579 (1992).
[6] M. S. Dresselhaus, G. Dresselhaus, and P. C. Eklund, *Science of Fullerenes and Carbon Nanotubes* (Academic Press Inc., San Diego, 1996).
[7] S. J. Tans *et al.*, Nature (London) **386**, 474 (1997).
[8] J. W. G. Wildör *et al.*, Nature (London) **391**, 59 (1998).
[9] R. Kuzuo, M. Terauchi, and M. Tanaka, Jpn. J. Appl. Phys. **31**, L1484 (1992).
[10] P. M. Ajayan, S. Ijima, and T. Ichihashi, Phys. Rev. B **49**, 2882 (1994).
[11] L. A. Bursill *et al.*, Phys. Rev. B **49**, 2882 (1994).
[12] R. Kuzuo *et al.*, Jpn. J. Appl. Phys. **33**, L1316 (1994).
[13] P. Petit *et al.*, Phys. Rev. B **56**, 9275 (1997).
[14] A. M. Rao *et al.*, Science **275**, 187 (1997).
[15] A. Thess *et al.*, Science **273**, 483 (1996).
[16] A. G. Rinzler *et al.*, Appl. Phys A (to be published); J. Liu *et al.* (to be published).
[17] J. Fink, Adv. Electron. Electron Phys. **75**, 121 (1989), and references therein.
[18] A. A. Lucas, L. Henrad, and Ph. Lambin, Phys. Rev. B **49**, 2888 (1994).
[19] M. F. Lin and K. W. K. Shung, Phys. Rev. B **50**, 17 744 (1994).
[20] M. F. Lin *et al.*, Phys. Rev. B **53**, 15 493 (1996).
[21] H. Romberg *et al.*, Synth. Met. **55-57**, 3038 (1993).
[22] As is often the case in EELS at high momentum transfers, contributions from the $q = 0$ spectrum reappear due to quasielastic scattering. This is the case here for $q \geq 0.5$ Å^{-1}.
[23] J. Fink and G. Leising, Phys. Rev. B **34**, 5320 (1986).
[24] Because of the presence of the quasielastic line at extremely low energies ($E < 0.4$ eV) EELS is unable to deliver directly an experimental value for $\epsilon_r(0)$. For the SWNTs we have taken $\epsilon_r(0)$ to be 100 ($q = 0.1$ Å^{-1}), which is arrived at from an average of the values for graphite in the plane [25] and perpendicular to the plane [H. Venghaus, Phys. Status Solidi **66**, 154 (1974)]. It is important to note, however, that the energy positions of the interband transitions in the optical conductivity are essentially unchanged if a metallic extrapolation to zero energy is assumed (data not shown).
[25] K. Zeppenfeld, Z. Phys. **243**, 229 (1971).
[26] J. J. Ritsko and E. J. Mele, Phys. Rev. B **21**, 730 (1980).
[27] E. Sohmen and J. Fink, Phys. Rev. B **47**, 14 532 (1993).